Mechanism of the Fe^{3+} Reduction at Low Temperature for $LiFePO_4$ Synthesis from a Polymeric Additive

N. Ravet,[†] M. Gauthier,[‡] K. Zaghib,[§] J.B. Goodenough,[||] A. Mauger,*[,⊥] F. Gendron,[#] and C.M. Julien[#]

Département de Chimie, Université de Montréal, Montréal, Québec, Canada 3HC 3J7, Phostech Lithium, 135-D chemin du Tremblay, Boucherville, QC, Canada J4B7K4, [3]Institut de Recherches d'Hydro−Québec, 1800 Boulevard Lionel-Boulet, Varennes, Québec, Canada J3X 1S1, The University of Texas at Austin, 1 University Station, C2200, Austin, Texas 78712, Département Mathématiques, Physique, Planète et Univers (MPPU), CNRS, Campus Boucicaut, 140 rue de Lourmel, 75015 Paris, France, and Institut des Nano-Sciences de Paris, CNRS-UMR 7588, Université Pierre et Marie Curie, 140 rue de Lourmel, 75015 Paris, France

Received February 20, 2007. Revised Manuscript Received March 16, 2007

Comparison is made between the use of either a carbon powder or a polymer additive to the precursors in the synthesis of $LiFePO_4$ from the Fe(III) compound $FePO_4(H_2O)_2$ and Li_2CO_3. The evolution of the structural properties and phase purity with temperature and time have been monitored at all length scales by X-ray diffraction, Fourier transformed infrared spectroscopy, and magnetic susceptibility. The reactor temperature was decreased to 300 °C to investigate the early stages of the reaction. Formation of crystalline $LiFePO_4$ begins in the range 300−400 °C only if the polymer is used as the carbonaceous additive. This $LiFePO_4$ formation is made possible by the reduction of Fe(III) species by gases such as H_2 or gaseous hydrocarbons evolved during the calcination of the polymer. Moreover, decomposition of the polymer results in a carbonaceous deposit on the surface of the $LiFePO_4$ particles. An $Li_3Fe_2(PO_4)_3$ impurity found after sintering at 400 °C for 4 h was greatly reduced after sintering at 400 °C for 24 h, and phase-pure $LiFePO_4$ was attained at 700 °C. Where the solid carbon powder was used as the reducing agent, no Fe(II) species could be detected after sintering at 400 °C. Carbothermal reduction of Fe(III) is ruled out in this temperature range.

1 Introduction

Among the promising materials for positive electrodes of Li-ion rechargeable batteries, lithium iron phosphate $LiFePO_4$ has attracted huge interest since the pioneering work of Padhi et al.[1] It exhibits a slightly lower voltage than the widely used commercial $LiCoO_2$, but it has a higher specific capacity (∼170 mAh/g) and an increased safety. The 3.45 V potential vs Li^+/Li^0, which is higher than that of previously known iron-based cathode materials, comes from the inductive effect of the $(PO_4)^{3-}$ phosphate group that lowers the energy of the Fe^{3+}/Fe^{2+} redox couple in the olivine structure environment. In addition, it is inexpensive and nontoxic. The major drawback of $LiFePO_4$ is its low electronic conductivity, which may result in a loss of capacity during high-rate discharge, a major inconvenience in power-demanding applications such as hybrid electric vehicles. That is why a great deal of effort has been made to improve the electric conductivity. This goal has been achieved either by adding carbon as an additive or by surface coating of the $LiFePO_4$ particles with thin layers of carbon.[1−4]

Ravet et al. reported different ways to obtain carbon deposits on $LiFePO_4$ from the decomposition of organic substances in a one- or two-step synthesis.[2−4] It was further demonstrated that pyrolyzing organic additive can simultaneously reduce Fe(III) to Fe(II) and the organic material to carbon.[5] The result leads to electronically conductive particles with higher capacity, improved cyclability, and better kinetics. In addition, the materials prepared at 700 °C with such a carbon additive turn out to be free of Fe(III) impurities. Without the carbon additive, nanoparticles of maghemite (γ-Fe_2O_3) were detected.[6] This is proof that a second and fortunate effect of the use of an organic carbon additive is a reduction of Fe(III) species that prevents the formation of ferrite or other complex oxide compounds involving Fe(III) ions.[7] The reason for this secondary effect, however, has not yet been clarified. There has been a temptation to attribute this effect to a carbothermal reduction.[7−9] However, we know

* Corresponding author. E-mail: mauger@ccr.jussieu.fr.
[†] Université de Montréal.
[‡] Phostech Lithium.
[§] Institut de Recherches d Hydro Québec.
[||] The University of Texas at Austin.
[⊥] CNRS, Campus Boucicaut.
[#] Université Pierre et Marie Curie.

(1) Padhi, A. K.; Nanjundaswamy, K. S.; Goodenough, J. B. *J. Electrochem. Soc.* **1997**, *144*, 1188.
(2) Ravet, N.; Chouinard, Y.; Magnan, J. F.; Besner, S.; Gauthier, M.; Armand, M. *J. Power Sources* **2001**, *503*, 97−98.
(3) Ravet, N.; Abouimrane, A.; Armand, M. *Nat. Mater.* **2003**, *2*, 702.
(4) Ravet, N.; Besner, S.; Simoneau, M. Vallée, A. Armand, M.; Magnan, J. F. U.S. Patent 6 962 666 and 6 855 273.
(5) Armand, M.; Gauthier, M.; Magnan, J.-F.; Ravet, N. World Patent WO 02/27823 A1 2002.
(6) Ait Salah, A.; Mauger, A.; Julien, C. M.; Gendron, F. *Mater. Sci. Eng., B* **2006**, *129*, 232.
(7) Ait-Salah, A.; Zaghib, K.; Mauger, A.; Gendron, F.; Julien, C. M. *Phys. Status Solidi, A* **2006**, *203*, R1.
(8) Barker, J.; Saidi, M. Y.; Swoyer, J. L. *J. Electrochem. Soc.* **2003**, *150*, A684.

10.1021/cm070485r CCC: $37.00
Published on Web 04/24/2007

from the iron industry that the reduction of Fe^{3+} by carbon is efficient only at high temperature, typically 1000 °C. Of course, the kinetics of the reactions involving carbon might be influenced by the presence of the precursors of $LiFePO_4$ in the course of the sample preparation, but the fact that the reduction reaction occurs at quite low temperatures, 300−400 °C, and that the sintering temperature does not exceed 700 °C makes the existence of any carbothermal effect very questionable.[10]

One aim of this present work is to establish whether the reduction of Fe(III) impurities occurs via a carbothermal reaction or by the action of a reductive atmosphere created by the pyrolytic degradation of the organic carbon additive. For this purpose, we have chosen to investigate the reduction mechanism during the synthesis of $LiFePO_4$ prepared from Fe(III) starting material ($FePO_4$) at different temperatures under an argon atmosphere. The structural properties were determined from X-ray diffraction (XRD), Fourier transform infrared (FTIR) spectroscopy, and magnetometry. The combination of these different measurements gives access to the structure and impurity content at any length scale, from the long-range down to the nanometer scale.[6,11] The use of Mössbauer might also quantify the Fe(III) ions, but the advantage of the full investigation of the magnetic properties is that it allows us to identify the nature of the Fe(III)-related impurity phases that poison the material.

2. Experimental Section

2.1. Sample Synthesis. Two blends, containing stoichiometric quantities of $FePO_4(H_2O)_2$ (from Budenheim, grade E53-81) and Li_2CO_3 (from Lintech, 99.9%) were prepared in stoichiometric ratios. In addition, the first blend contained a stoichiometric amount of carbon (Shawinigan black) according to the formation of CO (i.e., 0.05 mole of C per mole of $FePO_4(H_2O)_2$). After ball milling in isopropyl alcohol (IPA) overnight, the blend was dried, thoroughly mixed by hand, and pressed into pellets. The second blend contained around 5% by weight of a polymeric carbon additive, polyethylene-*block*-poly(ethylene glycol) 50% ethylene oxide (from Aldrich). It was mixed overnight in IPA and used as obtained after drying. In this case, the polymer sticks particles of the reactant together so there was no need to pelletize. All syntheses were carried out under flowing argon. Note that the carbon source could provide the $LiFePO_4$ powder with a carbonaceous deposit after pyrolysis and that such a powder pressed at 3750 kg/cm^2 at room temperature[5] presents an electronic conductivity much higher than 1×10^{-8} S/cm. Other elements that can be present are hydrogen, oxygen, and nitrogen, as long as they do not interfere with the chemical inertia of the carbon.[4] Preferred polymeric additives include, but are not limited to, hydrocarbons and their derivatives, especially those comprising polycyclic aromatic moieties, e.g., polyolefins, polybutadienes, polyvinyl alcohol, etc.[4]

Hereafter, the products obtained by the calcination of the blends are designated LFP samples in contrast to the well-crystallized triphylite $LiFePO_4$. The synthesis parameters (reducing agent, atmosphere, sintering time, and temperature) are recorded in Table 1.

Table 1. Growth Parameters for the Lithium Iron Phosphate Samples

sample	precursor and carbon additive mixing	thermal treatment: T (°C)	thermal treatment: duration (h)	thermal treatment: atmosphere
LFP1	$FePO_4(H_2O)_2$, Li_2CO_3, carbon	400	4	argon
LFP2	$FePO_4(H_2O)_2$, Li_2CO_3, polymer	300	4	argon
LFP3	$FePO_4(H_2O)_2$, Li_2CO_3, polymer	400	4	argon
LFP4	$FePO_4(H_2O)_2$, Li_2CO_3, polymer	400	24	argon

2.2. Apparatus. The crystal structure of LFP samples was analyzed by X-ray diffraction (XRD) with a Philips X'Pert apparatus equipped with a CuK_α X-ray source ($\lambda = 1.5406$ Å). XRD measurements were collected in the 2θ range 10−80°. FTIR absorption spectra were recorded with a Fourier transform interferometer (model Bruker IFS113v) in the wavenumber range 150−1400 cm^{-1} at a spectral resolution of 2 cm^{-1}. The samples were ground to fine powders and dispersed onto a CsI pellet in the proportion (1:300).

Magnetic measurements (susceptibility and magnetization) were carried out with a fully automated magnetometer (MPMS-5S from Quantum Design) with an ultra-sensitive superconducting quantum interference device (SQUID) in the temperature range 4−300 K. Powders were placed into a small plastic vial, put into a holder, and finally inserted into the helium cryostat of the SQUID apparatus. The temperature dependence of the magnetization data was recorded according to two procedures: zero-field cooling (ZFC) and field cooling (FC). In the ZFC procedure, the sample was first cooled down in the absence of a magnetic field and a magnetic field $H =$ 10 kOe was then applied; the ZFC magnetic susceptibility is defined as $M(T)/H$, where M is the magnetization measured upon heating. In the FC experiments, the same magnetic field was applied first at room temperature; the FC susceptibility was measured upon cooling. Magnetic curves $M(H)$ have been measured in an applied magnetic field in the range 0−30 kOe.

3. Results and Discussion

3.1. Structural Properties. *(a) X-ray Diffraction Analysis.* The XRD patterns of the four LFP samples prepared following the procedures described in Section 2 and Table 1 are shown in Figure 1. The LFP1 product exhibits an XRD pattern essentially flat, showing that the addition of carbon powder did not allow any crystallization of the $LiFePO_4$. To the contrary, the XRD pattern of the sample LFP3 shows that the $LiFePO_4$ is well-crystallized. Both samples have been prepared with the same precursors at the same temperature $T_s = 400$ °C; the only difference is the carbon additive that is solid carbon powder for LFP1, and the polymer for LFP3. This result gives a first proof that the carbon is not the efficient agent that allows the triphylite phase to grow up. The synthesis has then been made possible only by the hydrogen that is the common ingredient present in the polymer we have used here and all the other organic compounds that have already proved their efficiency for that purpose. As a consequence, we shall now focus attention to the samples LFP2-4, prepared in presence of the polymer. To illustrate the early stages of the $LiFePO_4$ synthesis, we have detailed in Figure 2 the XRD spectra of the samples LFP2,3 sintered for 4 h at 300 and 400 °C, respectively. The pattern of the sample sintered at 300 °C (LFP2) is actually dominated by the pattern characteristics of $Li_3Fe_2(PO_4)_3$[12,13] (hereafter referred to as NASICON, as it has the

(9) Quan Zhu, B.; Hai Li, X.; Xing Wang, Z.; Jun Guo, H. *Mater. Chem. Phys.* **2006**, *98*, 373.
(10) Ait Salah, A.; Mauger, A.; Zaghib, K.; Goodenough, J. B.; Ravet, N.; Gauthier, M.; Gendron, F.; Julien, C. M. *J. Electrochem. Soc.* **2006**, *153*, A1692.
(11) Yang, S.; Zavalij, P. Y.; Whittingham, M. S.; *Electrochem. Commun.* **2001**, *3*, 505.

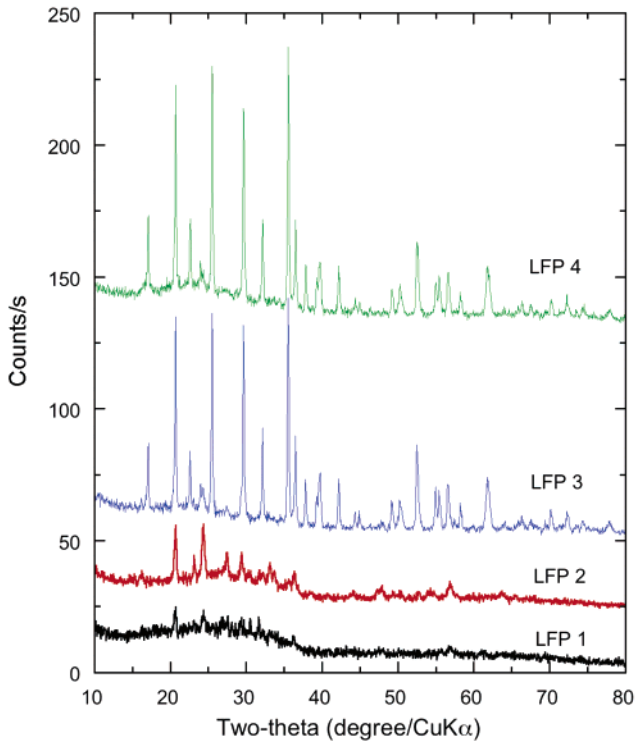

Figure 1. XRD patterns of the lithium iron phosphates prepared from $FePO_4 \cdot 2H_2O$ and Li_2CO_3 in various conditions. LPF1 was grown with solid carbon powder, whereas LFP2,3,4 samples were synthesized with a polymeric additive and sintered at 300 °C for 4 h, 400 °C for 4 h, and 400 °C for 24 h, respectively. The formation of the $LiFePO_4$ olivine framework occurred in the range 300−400 °C.

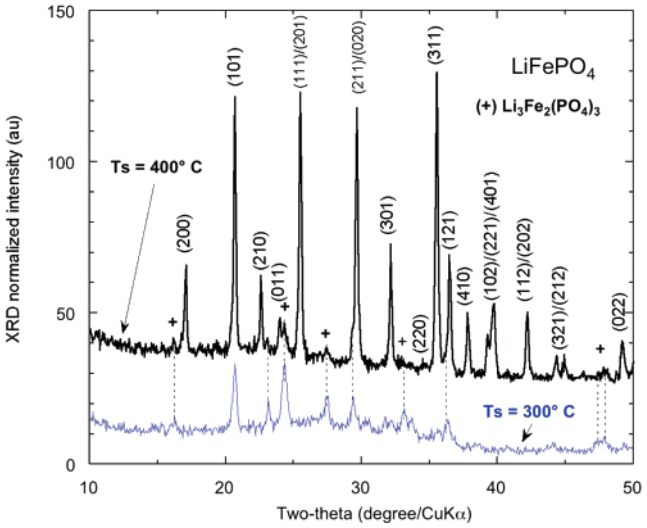

Figure 2. Detailed XRD patterns showing a comparison between the diagrams for LFP2 and LFP3 sintered for 4 h at 300 and 400 °C, respectively. The $Li_3Fe_2(PO_4)_3$ phase is evidenced by the lines marked by vertical broken lines and (+) symbols. The other lines are those of the triphylite phase; they are indexed in the orthorhombic *Pnma* system.

NASICON framework). The Bragg peaks of $LiFePO_4$ (see for instance ref 7 and references therein) emerge from the background, but their intensity remains small, giving evidence that the $LiFePO_4$ formation has just started at this temperature. On the other hand, the XRD pattern of the sample sintered at T_s = 400 °C shows this value of T_s is now large enough that a large quantity of $LiFePO_4$ has crystallized. The lines associated with the triphylite phase have grown up at the expense of those of the NASICON phase. In the same way, the comparison between the XRD spectra of the LFP3 and LFP4 samples show that the longer time spent at T_s = 400 °C in the LFP4 sample (24 instead of 4 h) still increases the amount of the $LiFePO_4$ phase at the expense of the $Li_3Fe_2(PO_4)_3$ phase. The quantitative amount of NASICON in the samples will be determined by magnetic measurements in next sections. At his stage, let us just note that $Li_3Fe_2(PO_4)_3$ contains Fe(III) ions while the iron is divalent in pure $LiFePO_4$. Therefore, the dominant amount of the NASICON phase in the LFP2 sample is a proof that the polymer failed to reduce Fe(III) species at T_s = 300 °C, whereas the hydrogen coming from the polymer is much more efficient at T_s = 400 °C. At this last temperature, the kinetics of the reduction of Fe(III) is faster, but still slow enough so that the reduction of the NASICON phase can be followed at the scale of few hours. This result is confirmed and quantified by FTIR spectroscopy and SQUID magnetometry analysis described in the next sections.

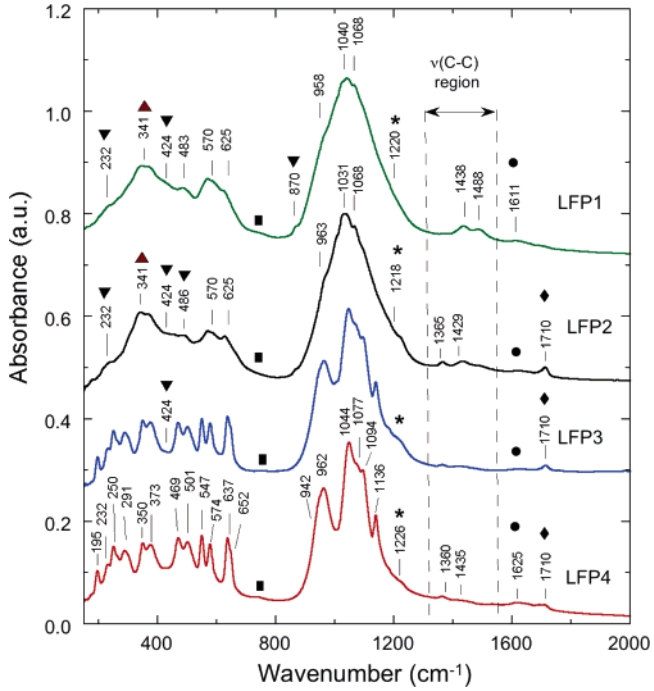

Figure 3. FTIR absorption spectra of lithium iron phosphate materials. LFP powders were dispersed in anhydrous CsI in a 300:1 ratio for easy measurements in the far-infrared region. Spectra of LFP3 and LFP4 powders show infrared bands typical of the $LiFePO_4$ olivine framework. Extrinsic vibrations are marked by different symbols: ■, $LiFeP_2O_7$; *, $Li_3Fe_2(PO_4)_3$; ▼, Li_3PO_4; ▲, $FePO_4$; ◆, (−HC═CH_2) vinyl group of the polymer; ●, δ(O−H) bending mode coming from the $FePO_4 \cdot 2H_2O$ precursor, whereas the other bands are associated with ν(C−C) vibrations.

(b) FTIR Spectroscopy. The structure at the molecular size scale has been investigated by FTIR absorption experiments. The spectra of the samples are shown in Figure 3. The vibrational motions of LFP materials and the positions of the corresponding IR peaks have already been identified and

(12) Bykov, A. B.; Chirkin, A. P.; Demyanets, L. N.; Doronin, S. N.; Genkina, E. A.; Ivanov-shits, A. K.; Kondratyuk, I. P.; Maksimov, B. A.; Mel'nikov, O. K.; Muradyan, L. N.; Simonov, V. I.; Timofeeva, V. A. *Solid State Ionics* **1990**, *38*, 31.
(13) Ait Salah, A.; Jozwiak, P.; Garbarczyk, J.; Gendron, F.; Mauger, A.; Julien, C. M. *Electrochem. Soc. Proc.* **2005**, *20*, 173.

discussed.[14,15] The vibrations can be divided into two classes that originate from the intramolecular vibrations of the PO_4^{3-}oxo-anion (T_d point group): the internal vibrations of PO_4 located in the range 1200−400 cm^{-1}, and external optical modes of PO_4 located below 400 cm^{-1}.[16] In the spectral region of the internal modes of the phosphate anion, the symmetric ν_1 and asymmetric ν_3 stretching modes are located in the high-wavenumber region (900−1150 cm^{-1}) well-separated from the bands due to the asymmetric ν_4 and symmetric ν_2 bending vibrations that appear in the low-wavenumber region (400−650 cm^{-1}).[17] As expected, these fundamental vibrations of the PO_4^{3-}oxo-anions dominate all the vibrational spectra of the samples (Figure 3). However, the richness of the spectra increases along the series LFP1−4.

Let us first consider the best-resolved FTIR spectrum of the LFP4 sample. The vibrations of the PO_4^{3-}units are split into many components due to the correlation effect induced by the coupling with of Fe−O units in the material. This richer spectrum then gives evidence that this sample is well-crystallized. Indeed, the positions of the internal modes in the spectrum of the LFP4 samples are in good agreement with those of the $LiFePO_4$ olivine. Considering the stretching vibrations, the ν_1 symmetric modes are located at 942 and 962 cm^{-1}, whereas the ν_3 asymmetric stretching modes appear at 1044, 1077, 1094, and 1136 cm^{-1}. This part of the spectrum matches (within 2 cm^{-1}) the spectrum observed for $LiFePO_4$ fully crystallized after sintering at 700 °C.[8] This match is also true for the part of the spectrum in the spectral range below 660 cm^{-1}. The positions of the modes are in quantitative agreement with those listed in Table 1 in ref 15 for a pure $LiFePO_4$ olivine crystal and those of our fully crystallized samples after sintering at 700 °C.[18] In this range, the IR bands are combinations of the O−P−O ν_4 and ν_2 bending vibrations and Li vibrations.[14,15] In particular, the mode at 232 cm^{-1} is the local mode of the lithium ions that undergo translation vibration inside the cage formed by the six nearest-neighbor oxygen atoms.[19] This mode appears in the spectrum of LFP1 because it is infrared-active not only in $LiFePO_4$ but also in Li_3PO_4 material. These low-frequency modes below 660 cm^{-1} are thus particularly sensitive to the local environment of the lithium and the local structure of the olivine lattice. The multiplicity of the fundamental modes in this range is due to the correlation $T_d \rightarrow C_s \rightarrow C_{2h}$ from point group to crystal. To be more specific, internal modes are split as a consequence of two effects: the site-symmetry effect due to an electric crystal field of symmetry lower than tetrahedral acting on the molecule and the correlation effect due to the presence of more than one molecular group in the crystal unit cell. Therefore, the FTIR absorption experiments show that the LFP4 sample is very well crystallized.

The only feature that distinguishes the spectrum from pure $LiFePO_4$ is the appearance of two weak spectral features at 741 and 1226 cm^{-1} that cannot arise from the $LiFePO_4$ internal vibrations. The former is attributed to the asymmetric ν'_{as} stretching mode of P−O−P bridges of $LiFeP_2O_7$,[20,21] which indicates the presence of a small amount of this material within the LFP4 structure. The P−O−P bridge of the $P_2O_7^{4-}$ pyrophosphate group may be considered as an independently vibrating unit within the limits of this approximation; its stretching frequencies depend not only on the bridging θ_{POP} angle but also on the force constant of the P−O bond of the bridge. For the staggered configuration with a nonlinear θ_{POP} angle, the frequency of the ν'_{as}(P−O−P) vibration appears at 763 cm^{-1} for $LiFeP_2O_7$.[20,21] The second additional feature at 1226 cm^{-1} is attributed to the presence of $Li_3Fe_2(PO_4)_3$ that is mixed with the triphylite phase. Lantern units building the $Li_3Fe_2(PO_4)_3$ lattice give rise to infrared bands in the range 1150−1250 cm^{-1},[20] which are attributed to the stretching vibrations of terminal PO_3 units because the NASICON phase shows the same vibrational modes that are observed in $R(PO_3)_3$ metaphosphates (R = Ga, In, Y, Sm, Gd, Dy) in the range 1230−1280 cm^{-1}.[22]

Let us now turn to the FTIR spectra of the other samples. The modes in the LFP3 sample are significantly broader than in the case of LFP4. This broadening is evidence of a decrease in the lifetime of the phonons and thus of the existence of defects that break the periodicity of the lattice inside the $LiFePO_4$ crystallites, as was also detected by the broader peaks in the XRD spectrum. The band associated with $Li_3Fe_2(PO_4)_3$ at 1226 cm^{-1} has increased, so that the amount of the NASICON impurity phase has increased. Note that the only difference between LFP4 and LFP3 samples prepared with the polymer as the carbon additive is the duration of the sintering at 400 °C. The larger concentration of NASICON in the LFP3 sample is then a proof that the kinetics of the Fe(III) reduction by the gaseous elements issued from the polymer are slow at 400 °C and that this reduction still goes on at the scale of hours at this temperature. We shall quantify this kinetics with magnetic measurements in the next section. Also, a close inspection of the LFP3 spectrum shows a weak IR band at 424 cm^{-1} that we attribute to a small amount of Li_3PO_4.[23,24]

The FTIR spectrum of the LFP2 sample is even broader than that of the LFP3 sample, confirming the poorer crystallinity of LFP2. Furthermore, one can no longer distinguish between ν_3 and ν_1 stretching modes. The broad band at 341 cm^{-1} is characteristic of the $FePO_4$ structure; the existence of this band is not detected in the LFP3,4 samples.[16] The Fe is trivalent in $FePO_4$, so the detection of this impurity phase in addition to the NASICON phase shows that the polymer failed to reduce efficiently Fe(III)

(14) Paques-Ledent, M. T.; Tarte, P. *Spectrochim. Acta, A* **1974**, *30*, 673.
(15) Burma, C. M.; Frech, R. *J. Electrochem. Soc.* **2004**, *151*, 1032.
(16) Zaghib K.; and Julien, C. M. *J. Power Sources* **2005**, *142*, 279.
(17) Tarte, P. *Spectrochim. Acta* **1964**, *20*, 238.
(18) Julien, C.; Zaghib, K.; Mauger, A.; Massot, M.; Ait-Salah, A.; Selmane, M.; Gendron, F. *J. Appl. Phys.* **2006**, *100*, 1.
(19) Ait Salah, A.; Jozwiak, P.; Zaghib, K.; Garbarczyk, J. Gendron, F.; Mauger, A.; Julien, C. M. *Spectrochim. Acta, Part A* **2006**, *65*, 1007.
(20) Ait Salah, A.; Jozwiak, P.; Garbarczyk, J.; Benkhouja, K.; Zaghib, K.; Gendron, F.; and Julien, C. M. *J. Power Sources* **2005**, *140*, 370.
(21) Julien, C. M.; Ait-Salah, A.; Gendron, F. *Electrochem. Soc. Proc.* **2006**, *501*, 1343.
(22) Alieva, D.; Koacheva, D.; Petkov C.; and Bogachev, G. *J. Raman Spectrosc.* **2001**, *32*, 893.
(23) Tarte, P. *J. Inorg. Nucl. Chem.* **1967**, *29*, 915.
(24) Ait Salah, A.; Jozwiak, P.; Garbarczyk, J.; Gendron, F.; Mauger, A.; Julien, C. M. *Electrochem. Soc. Proc.* **2005**, *20*, 103

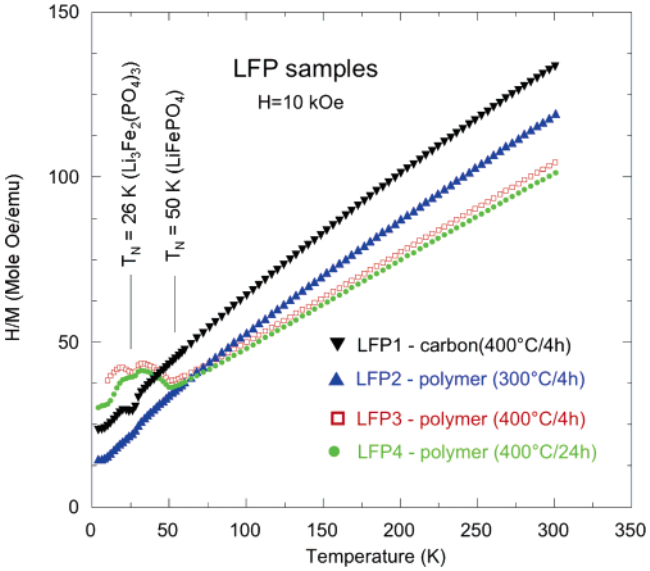

Figure 4. Plot of the magnetic susceptibility H/M for LFP samples prepared in the various conditions given in Table 1. LFP3 and LFP4 samples show the Néel temperatures of both the $LiFePO_4$ olivine phase ($T_N = 50$ K) and of $Li_3Fe_2(PO_4)_3$ phase ($T_N = 26$ K).

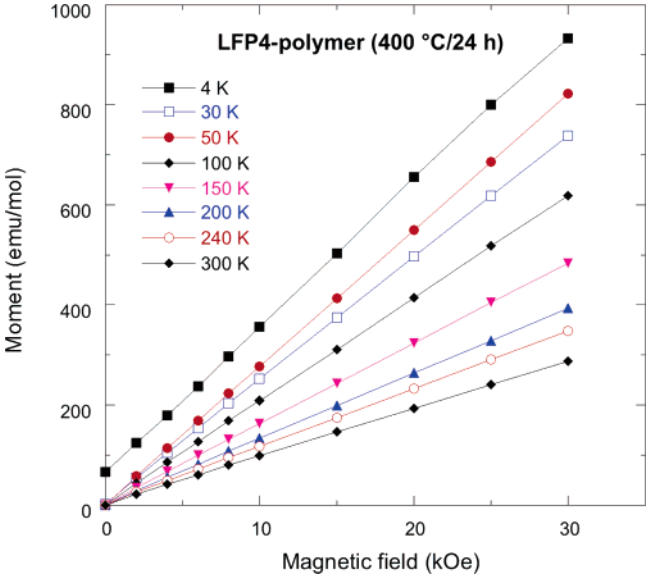

Figure 5. Isothermal magnetization curves $M(H)$ for the LFP sample prepared from polymeric additive and heated at 400 °C for 24 h.

at 300 °C. This observation is actually expected, because the lower value of T_s can only result in a critical slowingdown of the reduction process.

Finally, the structures of the LFP1 spectrum are even more smeared out because the carbon is of no help and does not react with the precursor elements of $LiFePO_4$ to synthesize this material.

The FTIR spectra of all the LFP1−LFP4 samples present some extra bands of weak intensity in the spectral range above 1300 cm^{-1}. These bands are due to the remaining hydrocarbon species. For instance, two bands in the spectral range 1300−1500 cm^{-1} are attributable to the ν(C−C) vibrations, their exact position depending on the environment. The C═C stretching mode of the vinyl groups (−HC═CH_2) appears at 1710 cm^{-1}.[25] This C═C bond is pre-existent in the polymer; it is not formed during the sintering of the sample. In particular, we can see in Figure 3 that these peaks do not exist in the LFP1 sample where the polymer has been replaced by carbon. Another IR band characteristic of the δ(O−H) bending mode is observed at 1610−1625 cm^{-1} due to the use of the hydrated $FePO_4$ precursor material. All the infrared bands characteristic of the hydrocarbon species are deleted on firing the material above 400 °C,[18,19] but their existence at $T_s = 400$ °C shows that the polymer has not been completely dissociated at this temperature.

3.2. Magnetic Properties. Figure 4 shows the temperature dependence of the reciprocal magnetic susceptibility, $\chi_m^{-1}(T)$, for the different samples measured in an applied field $H =$ 10 kOe. The $\chi_m^{-1}(T)$ curves can also be divided into two different classes. The samples LFP3 and LFP4 show a peak of magnetic susceptibility at $T_N = 50$ K, which is known to be the Néel temperature of pure crystallized $LiFePO_4$.[26] Therefore, these samples are well-crystallized and the impurities are diluted so that neither structural defects nor the impurities can impede the propagation of long-range spin correlations that are responsible for the onset of the antiferromagnetic ordering. On the other hand, the monotonous and continuous variation of $\chi_m^{-1}(T)$ in the vicinity of 50 K for the LFP1 and LFP2 samples show that the spin correlation length is not limited by thermal fluctuations, but by the distance between defects and impurities, and this average distance is so small that the spin correlations are always short-range, preventing the system from developing long-range magnetic order. That is the reason why the transition to the antiferromagnetic phase at 50 K can be observed only in the well-crystallized (LFP3, LFP4) samples.

A feature common to all the samples is an anomaly in the $\chi_m^{-1}(T)$ curves at 26 K that is characterized by a sharp decrease in $\chi_m^{-1}(T)$ upon cooling through this temperature. This feature signals the onset of a spontaneous magnetization at this temperature; it is corroborated by the magnetization curves $M(H)$ of Figure 5 taken at different temperatures in the range 4−300 K for the LFP4 sample as an illustration. The curves are linear in H down to 30 K, which eliminates any maghemite impurity phase.[6] On the other hand, the onset of a spontaneous magnetization at 26 K results in a nonvanishing magnetization in the limit $H \rightarrow 0$ at lower temperatures, as is illustrated by the curve at $T = 4$ K in Figure 5. This onset of a spontaneous magnetization at 26 K is the signature of the weak ferromagnetic component of $Li_3Fe_2(PO_4)_3$ at this temperature.[27,28] As stated in the previous section, this NASICON impurity phase has been detected together with the $LiFeP_2O_7$ by FTIR in our LFP samples. To determine the amount of these impurity phases, we have measured the $\chi_m^{-1}(T)$ curves of $Li_3Fe_2(PO_4)_3$ and $LiFeP_2O_7$ samples under the same conditions (i.e., $\chi_m = M/H$, with M measured in a magnetic field $H = 10$ kOe). The preparation

(25) Colthup, N. B.; Daly, L. H.; Wiberley, S. E. *Introduction to Infrared and Raman Spectroscopy*; Academic Press: New York, 1964.
(26) Santoro, R.; Newnham, R. E. *Acta Crystallogr.* **1967**, *22*, 344.
(27) Goni, A.; Lezama, L.; Moreno, N. O.; Fournes, L.; Olazcuaga, R.; Barberis, G. E.; Tojo, T. *Chem. Mater.* **2000**, *12*, 62.
(28) Anderson, A. S.; Kalska, B.; Jonsson, P.; Haggstrom, L.; Nordblad, P.; Tellgren, R.; Thomas, J. O. *J. Mater. Chem.* **2000**, *10*, 2545.

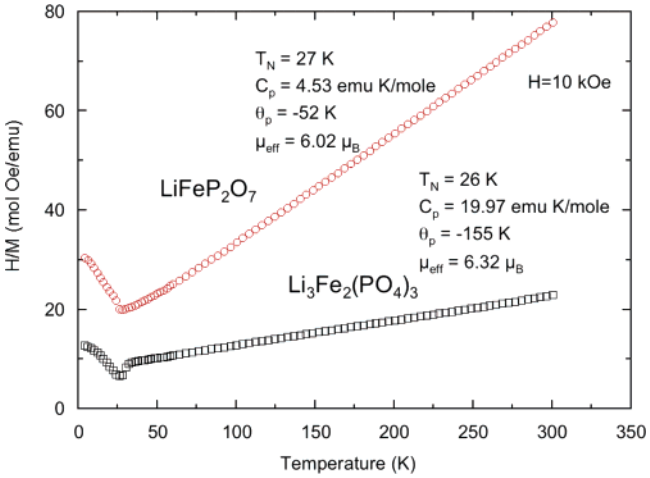

Figure 6. Plot of the magnetic susceptibility H/M for Fe(III)-containing LFP phases. $LiFeP_2O_7$ is an antiferromagnet below $T_N = 27$ K, whereas $Li_3Fe_2(PO_4)_3$ is a weak ferrimagnet below $T_N = 26$ K.

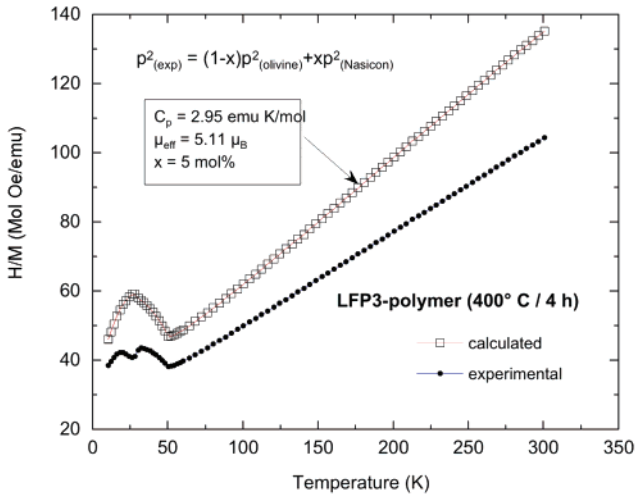

Figure 7. Plots of the temperature dependence of the curve H/M for the LFP3 sample heated at 400 °C for 4 h. Pen squares represent the calculated data from eq 3, namely after subtraction of the contribution of the $Li_3Fe_2(PO_4)_3$ phase in concentration of 5 mol % in the product.

of these samples has been described elsewhere.[20,24,29] The result is reported in Figure 6. First of all, both of these materials exhibit a magnetic anomaly at the same temperature (within 1 K). However, $LiFeP_2O_7$ is antiferromagnetic,[29−31] whereas the NASICON has a weak spontaneous magnetization due to spin canting below 26 K.[28] The larger magnetic susceptibility of the NASICON phase means that the magnetic properties of our LFP samples are more sensitive to the presence of the NASICON phase than to the presence of a smaller amount of $LiFeP_2O_7$. For this reason, we now focus attention on the contribution of the NASICON impurity phase.

Besides the effect of the weak ferromagnetism at low temperature, the NASICON phase also alters the magnetic susceptibility at high temperature. The magnetization of the LPF samples at any magnetic field and any temperature can be written as the sum of the contribution of the impurity phases M_{imp} and the intrinsic contribution M_0 of $LiFePO_4$

$$M(H,T) = M_0(H,T) + M_{imp}(H,T) \quad (1)$$

This additive formula relies on the assumption that there is no magnetic interaction between the particles of NASICON and the host. We have argued elsewhere[6] that this is indeed the case even in the presence of magnetic particles of γ-Fe_2O_3 and Fe_2P in $LiFePO_4$. At high temperatures ($T > 200$ K), the magnetization is linear in H, as can be seen in Figure 5, and the $\chi_m^{-1}(T)$ curves are linear too, as can be seen in Figure 4. Therefore, the Curie−Weiss law applies even though eq 1 takes the form

$$\chi_m = [1 - (\sum_{imp} x_{imp})]C_0/(T + \theta_0) + \sum_{imp} x_{imp}C_{imp}/(T + \theta_{imp}) \quad (2)$$

where C_0 and θ_0 are the Curie constant and paramagnetic Curie temperature of pure $LiFePO_4$ and the label "imp" refers to the impurity species in concentration x_{imp}. Note that the summation of the impurities of the individual Curie−Weiss laws in the second term of eq 2 never reduces itself to a net Curie−Weiss law because the paramagnetic Curie temperature of any impurity is different from that of the host. Where the amount of impurities is too high, this effect is responsible for a nonlinear behavior of $\chi_m^{-1}(T)$ even where the magnetization of the sample is linear in H. This nonlinear behavior is indeed what we observed for the samples LFP1 and LFP2: for these two samples, the $\chi_m^{-1}(T)$ curves in Figure 4 clearly present a negative curvature.

On the other hand, the curvature is much smaller for the samples LFP3 and LFP4, which have fewer magnetic impurities. In this case, it is then technically possible to fit the $\chi_m^{-1}(T)$ curve according to a Curie law $\chi_m^{-1}(T) = (T + \theta)/C$, where $C = N\mu_{eff}^2/(3k_B)$ with N the number of effective magnetic moments μ_{eff}, although this is clearly an approximation that does not take properly into account impurity effects. The Curie−Weiss parameters deduced from such a fit are $\theta = -82 \pm 1$ K for both LFP3 and LFP4 samples with μ_{eff} 5.42 μ_B and 5.47 μ_B, respectively. This result is in agreement with former values of these parameters in $LiFePO_4$[26] that have always been determined by following this analysis in the past. This effective magnetic moment is actually larger than the value $\mu_{eff} = 5.22$ μ_B we have determined from the magnetic susceptibility curve $\chi_0(T)$ for $LiFePO_4$ samples that have been prepared with the same polymer additive but sintered at $T_s = 700$ °C. After such a heat treatment, we have determined that the Fe(III) is totally reduced; no impurity could be detected.[6] We can then regard this value of μ_{eff} as that of "pure" $LiFePO_4$ and can attribute the higher value of μ_{eff} in the LFP3, 4 samples to the impurity effects. According to this idea, eq 1 can be written

$$(1-x)c_0 = \chi_m - x\chi_{NASICON} \quad (3)$$

Because we know the susceptibility curves entering this equation, we just have to determine the only fitting parameter

(29) Ait-Salah, A.; Gendron, F.; Mauger, A.; Julien, C. M. *Electrochem. Soc. Proc.* **2005**, *11*, 113.
(30) Riou, D.; Nguyen, N.; Benloucif, R.; Raveau, B. *Mater. Res. Bull.* **1990**, *25*, 1363.
(31) Dai, D.; Wangbo, M.-H.; Koo, H.-J.; Rocquefelte, X.; Jobic, S.; Villesuzanne, A. *Inorg. Chem.* **2005**, *44*, 2047.

x so that eq 3 is fulfilled. In practice, we have used two distinct procedures. According to both of them, we calculate $\chi_0(T)$ from χ_m and $\chi_{NASICON}$ according to eq 3. In the first approach, we adjust x so that the value $\mu_{eff} = 5.22\ \mu_B$ deduced from the slope of $\chi_0^{-1}(T)$ at high temperature is restored. In the second procedure, we look for the parameter x that annihilates the anomaly at 26 K of the $\chi_0(T)$ due to the onset of the spontaneous magnetic moment in the NASICON impurities. These two determinations are independent because one of them amounts to a fit at high temperature whereas the other one concerns the low-temperature part of the magnetic susceptibility curve. The result, illustrated in Figure 7 for the LFP3 sample, is the same for the two procedures: $x = 5\%$ for the LFP3 sample and 1% for the LFP4 sample. Therefore, the fit that restores the correct value of μ_{eff} also removes the singular behavior at 26 K. This self-consistency of the two independent fitting procedures guarantees that the analysis and the determination of x are correct.

Because the only difference between LFP3 and LFP4 samples is the duration of the sintering treatment at 400 °C (4 h for LFP3, 24 h for LFP4), we can conclude that the amount of the NASICON impurity is reduced by a factor of 5 by increasing the time from 4 to 24 h at $T_s = 400$ °C.

4. Summary and Conclusions

Our investigation of the structural properties of products sintered at $T_s = 300$ °C and 400 °C completes a formal analysis of $LiFePO_4$ samples sintered at 700 °C.[18] Two different carbon additives were used along with $FePO_4(H_2O)_2$ and Li_2CO_3: a polymer and a solid carbon powder. With the polymeric compound, crystallization of $LiFePO_4$ starts at 300 °C; $LiFePO_4$ was already well-crystallized at $T_s = 400$ °C, and the amount of unreduced F(III) in an $Li_3Fe_2(PO_4)_3$ impurity phase decreased by a factor of 5 on firing for 24 h rather than 4 h at 400 °C. Moreover, a small and well-controlled amount of carbon coating on the $LiFePO_4$ particles can be made with an organic additive. On the other hand, the synthesis of $LiFePO_4$ crystals at 400 °C by the same process proved to be impossible when the organic compound is replaced by pure carbon, which implies that the carbon is inactive at such temperatures. In particular, no carbothermal reduction of Fe(III) was observed. These results allow us to conclude that reduction of Fe(III) occurs through a reaction with the gas-phase evolving from the calcination of the polymer. This is consistent with the chemistry of iron oxide that tells us the carbothermal reduction of iron can take place only above 1000 °C.[38] This is actually true not only for FeO (in which iron is divalent),[38] but also for Fe_2O_3 (in which iron is trivalent).[39] The sintering temperature used for the synthesis of $LiFePO_4$ is much smaller, and actually, sintering at $T_s \geq 800$ °C is prohibited because such high temperatures generate impurity phases such as Fe_2P that damage the electrochemical properties.

The good crystallinity of the LFP3 and LFP4 samples was evidenced not only by XRD, but also by the FTIR spectra. In particular, the low-wavenumber part of the absorption spectrum is very sensitive to the crystallinity, and the bending vibrations γ_2 and γ_4 present well-developed bands in samples LFP3 and LFP4 prepared at 400 °C, but not in samples LFP2 prepared at 300 °C. In the high-wavenumber range, the IR bands appear exactly at the same position for all the samples, even in those that were mainly amorphous, because the PO_4 tetrahedra retain very stable chemical bonds even in a vitreous phase.[20]

The magnetic susceptibility also provided a check on the nature of the products because long-range magnetic ordering is sensitive to the crystallinity as well as the compound formed. The magnetic susceptibility was also shown to be sensitive to the existence of magnetic impurities not detected by XRD as previously shown for Fe_2P impurities in $LiFePO_4$[6] and magnetite impurities in skutterdites.[32] Moreover, magnetic measurements could be used to determine the concentration of the $Li_3Fe_2(PO_4)_3$ impurities in the $LiFePO_4$ samples. This determination provided information on the kinetics of the reduction reaction at 400 °C, the concentration of the $Li_3Fe_2(PO_4)_3$ impurity decreasing by a factor of 5 on extending the sintering at 400 °C from 4 to 24 h.

Kinetic parameters such as the reaction order and rate constants can be estimated from the slope of the linear portion of the mass-loss curve of NASICON with time by using the chemical equations of Cho et al.[33] Although we have not sufficient data to pursue this analysis, our data show that magnetic experiments can be an efficient tool to study the kinetics of the reduction of an impurity phase. Conventional methods require a large amount of material.[34]Because of the pioneering work of Whittingham et al.,[35]hydrothermal methods have been successfully applied to the synthesis of $LiFePO_4$ in just a few hours by heating only above 175 °C.[36,37]This is also clear evidence that the use of the reductive H_2 atmosphere allows to enhance the kinetics of Fe(III) reduction. We have shown that synthesis of $LiFePO_4$ by a different process involving the presence of an organic compound is also the result of reduction of iron by hydrogen and hydrocarbon gases, but in our procedure, crystallization of $LiFePO_4$ starts only after heating above 300 °C. The reason is that we designed our synthesis to optimize carbon coating of the $LiFePO_4$ particles, not to optimize hydrothermal conditions. Optimization of the synthesis of $LiFePO_4$ for the cathode of a rechargeable lithium-ion battery will result from an optimization of both the hydrothermal conditions and the conditions for carbon coating. In this respect, the recent hydrothermal synthesis of $LiFePO_4$ by heating at 175 °C only in the presence of sugar as a (nonoptimized) carbon additive looks very

(32) Amornpitoksuk, P.; Ravot, D.; Mauger, A.; Tedenac, J. C. *J. Alloys Compd*. **2007**, in press.
(33) Cho, P.; Mattisson, T.; Lyngfelt, A. *Fuel* **2004**, *83*, 1215.
(34) Readman, J. E.; Olafsen, A.; Smith, J. B.; Blom, R. *Energy Fuels* **2006**, *20*, 1382.
(35) Yang, S.; Zavajil, P. Y.; Whittingham, M. S. *Electrochem. Commun*. **2001**, *3*, 505.
(36) Chen J.; Whittingham, M. S. *Electrochem. Commun*. **2006**, *8*, 855.
(37) Dokko, K.; Koizumi, S.; Kanamura, K. *Chem. Lett*. **2006**, 35, 338.
(38) L'vov, B. *Thermochim. Acta* **2000**, *360*, 109 and references therein.
(39) Lee, J.-J.; Lin, C.-I.; Chen, H.-K. *Metal. Mater. Trans*. **2001**, *32B*, 1035.

promising. However, the optimization of the preparation of the material as a cathode element of lithium batteries can only be a compromise for the following reason. We have discussed in a prior work the structural properties of the carbon deposit[18] and argued that the carbon coating is electronically conducting when the sintering temperature is $T_s = 700$ °C. Because conducting (amorphous graphitic) layers usually require still higher pyrolysis temperatures, it will be difficult to decrease T_s without damaging the electronic conductivity of the carbon deposit. Lower T_s will favor sp^3 bonding, leading to the formation of diamondlike insulating carbon layers. $T_s = 700$ °C should then be an optimized value when using a polymer as the agent to obtain a conducting carbon deposit. In addition, the polymer is responsible for a reduction of Fe(III), preventing the formation of impurity phases at this sintering temperature. It has been widely believed in the recent past that the carbothermal effect was responsible for this reduction. The present work shows that such is not the case.

CM070485R